

## IMPULSE FORCE CALIBRATION WITH DROPPED WEIGHT AND LASER VIBROMETER

*Yang Jun*<sup>1,2</sup>, *Cao Yiqing*<sup>1</sup>, *He Xuan*<sup>1</sup> and *Yin Xiao*<sup>1</sup>

<sup>1</sup>Changcheng Institute of Metrology & Measurement (CIMM), Beijing, China, [yangjun@cimm.com.cn](mailto:yangjun@cimm.com.cn)

<sup>2</sup>School of Instrument Science and Opto&electronics Engineering, Beihang University, Beijing, China

**Abstract:** One impulse force device is set up in CIMM to calibrate force transducers' sensitivities with dynamic method. The free falling weight impacts the calibrated force transducer to generate large-amplitude impulse force up to 200kN with (1~10)ms pulse duration, and one extra small inertia mass is installed on the top of the falling mass to generate small impulse force down to 20N. The impulse force is measured by laser interferometer to trace the force to mass, time and length. Several piezoelectric transducers are calibrated with the impulse force calibration device and the amplitude sensitivity's measurement repeatability is below 0.4%.

**Keywords:** Impulse force, Dynamic calibration, Dropped weight, Laser interferometer, Inertia mass

### 1. INTRODUCTION

Dynamic force measurement is more and more widely used, such as robot joints, precision machining control, structural impact test, material fatigue test[1]. Piezoelectric force transducer is specially used in the dynamic force measurement due to its excellent dynamic characteristics and high resolution, but static calibration is not suitable for it due to the charge leakage, which is much more notable for these integral electronic piezoelectric transducers. Therefore, their sensitivities need to be calibrated dynamically. For transducers mainly used to measure impulsive forces, the data from impulse force calibration can be directly applied to the test. Some methods and devices have been developed for transducers used in impact and crash testing[2~5].

The dynamic force measurement method based on the inertia force by laser interferometry is a hotspot in the development of dynamic force primary standards<sup>[6-7]</sup>. Beijing Changcheng Institute of Metrology & Measurement (CIMM) has also done in-depth study of this method and applied it to the sinusoidal force and impulse force calibration. This paper will introduce the impulse force calibration device developed by CIMM, which is based on the design of impulse force generator and laser interferometry, including the design of impulse force generator, measurement method with laser interferometry and main system error analysis, application of amplitude sensitivity calibration.

### 2. IMPULSE FORCE GENERATOR

Horizontal impact sources are now mostly used in the impulse force calibrations [2~5], which have the advantages of good controllability of amplitude and small lateral operation, but their structure and using are complicated. With the development of the dropped weight impact test machines, the controllability and lateral movement of impulse force generators based on dropped weight have been obviously improved. Because of the convenience of the impulse force generator with dropped weight, it is used in the impulse force calibration device of CIMM.

The principle of impulse force generator with dropped weight is shown in Figure 1. The free-falling weight (large mass,  $M$ ) impacts the calibrated force transducer mounted on the foundation through the waveform controller (buffer) to produce large amplitude impulse force. The main body of the dropped weight device was modified from a mature shock test device. Three weights of same size are made of titanium alloy, steel and tungsten alloy, which masses are 5.1665kg, 14.3299kg and 32.4424kg. The max lifting height is 1m.

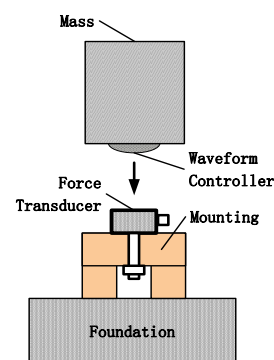


Fig.1. Principle of impulse force generator with dropped weight

For a half-sine waveform, the amplitude of the impulse force  $F_m$  has the following relation with the mass of the weight  $M$ , the lifting height  $h$ , and the pulse width  $T_w$  :

$$F_m \approx \frac{\pi \times M \times \sqrt{2gh}}{2T_w} \quad (1)$$

Where  $g$  is the local acceleration of gravity.

It can be seen from equation(1) that the amplitude of the generated impulse force can be adjusted by changing the lifting height and mass of the weight. The bouncing effect of the mass after the hit and the pulse width mainly are controlled by using of waveform controller with different materials and thickness. The materials of the waveform controllers include synthetic rubber, wool felt and cowhide. Of course the mass will hit the transducer several times and there is also several attenuating impulse force signals.

However, it is limited to obtain much higher amplitude by increasing the height, and there are difficulties to control the small impulse force's amplitude because the tiny change of the little height will make more remarkable change of the force amplitude .

Through a large number of experiments, the device can generate (1 ~ 200) kN impulse force, and the corresponding pulse width is about (10 ~ 1) ms. One 1kN and one 200kN impulse force waveforms are shown in Figure 2.

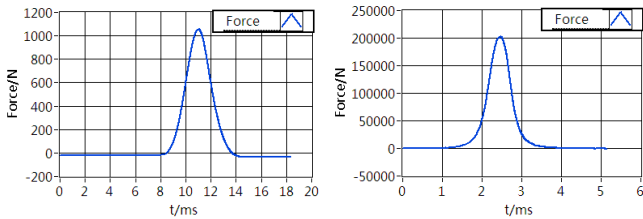


Fig.2. Waveforms of (1~200) kN impulse force

In order to obtain smaller impulse forces, an additional small mass ( $m$ ) is mounted on the top of the free-falling weight, which is shown in figure 3, and the calibrated force transducer is installed between the additional mass and the free-falling weight. When the free-falling weight is impacting the mounting, the force transducer is taking the inertial force from the additional mass. It is clear that the amplitude of the impulse force can be adjusted by the height of the falling and the additional mass. It is convenient to change the additional mass.

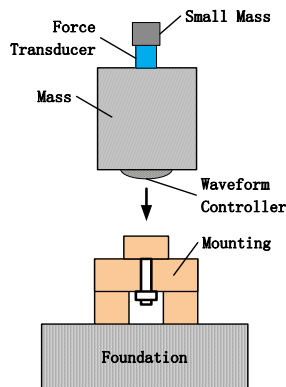


Fig.3. Principle of generating small-amplitude impulse force

By using additional masses of 109.35 g and 505.47 g respectively, 10 N to 1000 N impulse force can be get. And the pulse width is about (10 ~ 4) ms when just one waveform controller is used. The pulse width is more steadily than that of the large-amplitude impulse force and also can adjusted with different waveform controllers. One 10N and one 1000N impulse force waveforms are showed in figure 4.

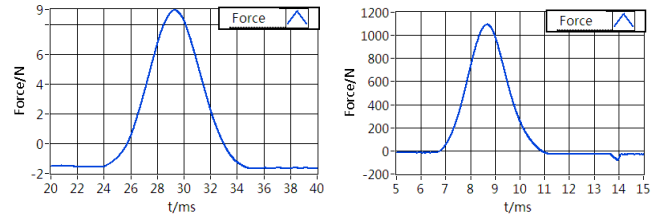


Fig.4. Waveforms of (10~1000) N impulse force

### 3. DYNAMIC FORCE MEASUREMENT WITH LASER VIBROMETER

The traceable measurement of dynamic force is a research hotspot in force metrology[8]. Motion mass' inertial force measured by laser interferometry is the main method used in the present traceable measurement of dynamic force<sup>[9~11]</sup>. First the inertial mass' motion parameters are measured by laser interferometry, and then the dynamic force is calculated based on Newton's second law. This method is also applied to this calibration device. The structure of the impulse force calibration device with a laser vibrometer is shown in figure 5. In order to constrain the large mass to reduce lateral movement and reduce the frictional resistance to the mass, an air bearing system (ABS) is used in conjunction with a cylindrical large mass.

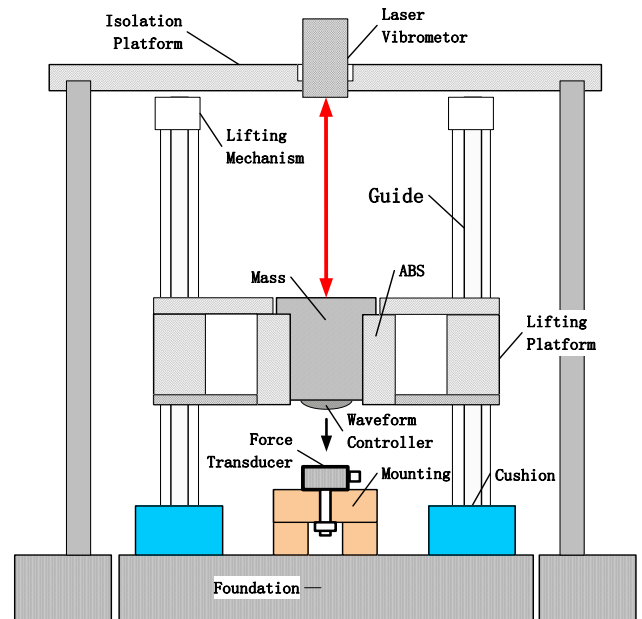


Fig.5. Structure of the impulse force calibration device with laser vibrometer

The measurement model of the large-amplitude impulse force is:

$$F = (M + m_1)(a + g) \quad (2)$$

Where  $m_1$ ,  $a$ , are the mass of the waveform controller and the mass' acceleration measured by the laser vibrometer.

When the additional small mass is applied for small-amplitude impulse force calibration, the laser vibrometer does not need to be adjusted, which is used to measure the acceleration of the small mass. An additional inertial force will take on the force transducer in this dynamic force calibration, which is from the transducer's partial mass

moving together with the small mass. The mass is sometimes called the transducer's efficient mass. Therefore the small-amplitude impulse force's measurement model is:

$$F = (m + m_0)(a + g) \quad (3)$$

Where  $m$  is the sum of the additional small mass and the mass of its connector, and  $m_0$  is the transducer's efficient mass.

However, there are the following several problems when equation (2) and equation (3) are used.

1) Disturbance of shocks to the laser vibrometer

In order to avoid or weaken the disturbance of vibrations or shocks to the laser vibrometer, isolated foundation and passive vibration isolation platform with isolation airbags are used. The isolated foundation's deep is more than 2m and the vibration isolation platform's height is about 2.7m.

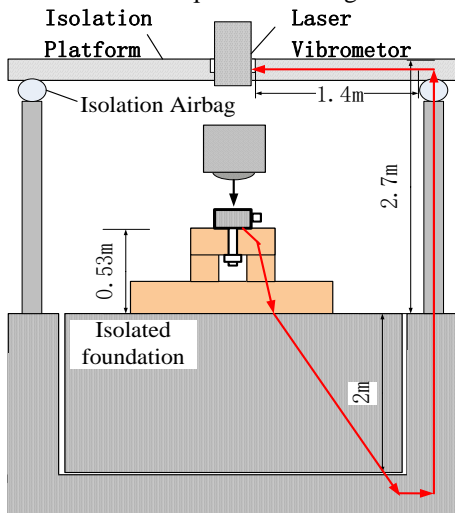


Fig.6. Structure of isolation system and transmission of shock wave

Assuming that the velocities of stress waves in concrete and steel are 4000m/s and 5200m/s, shock wave propagation from the force sensor to the laser vibrometer will take at least 1.9ms.

One three-component accelerometer was installed on the laser vibrometer, and the acceleration of the vibrometer ( $av$ ) was measured synchronously with the acceleration of the mass ( $a$ ) measured by laser vibrometer. Figure 7 shows the acceleration signals of the vibrometer when the shock wave is transmitted to the vibrometer. The three-component accelerations of the vibrometer are less than 0.2g, when the peak acceleration of the mass is about 540g. And from the time domain waveforms, the vibrometer measurement results have not received a significant impact from the shock. A large number of experimental results show that with the increase of pulse width, the relative vibration of the vibrometer is further reduced, which is always less than 0.05%, and there is no discernible effect on the laser vibrometer's measurement of the shock.

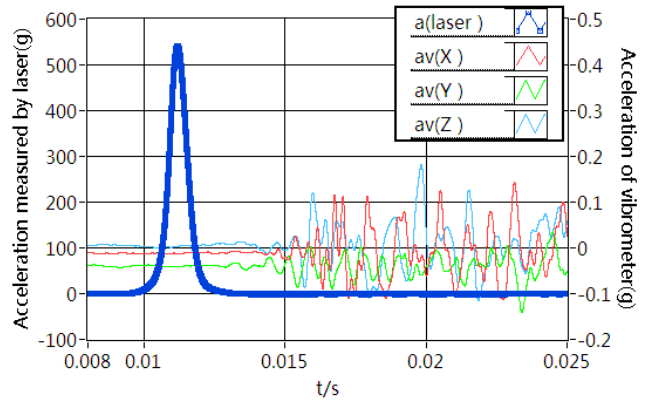


Fig.7. Accelerations of the mass by laser vibrometer and three-component accelerations of the vibrometer

2) Acceleration distribution of the inertial mass

The  $a$  in the equation (2) or equation (3) is the average acceleration of all effective inertial mass. But the laser vibrometer just measures the acceleration of one point on the top of the mass, which is always the central point. There is deviation between the two accelerations because there is acceleration distribution in the inertial mass and additional mass, especially for the large masses.

The finite element method was used to analyze the large masses' acceleration distribution of different materials and different impact loading modes. The three loading modes are shown in Fig.8. The maximum deviations of the top surface and the average acceleration are 1.28%, 1.07% and 0.95%, respectively, for point loading, local loading and surface loading.

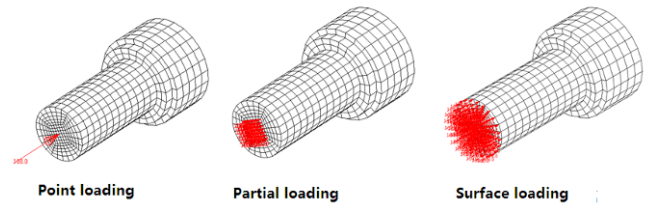


Fig.8. Three loading modes in FEM

At the same time, the acceleration distribution of the top surface of the large mass was measured, and five accelerometers were arranged in zigzag pattern, as shown in figure 9. The maximum acceleration deviation between center point and other points is 0.92%.

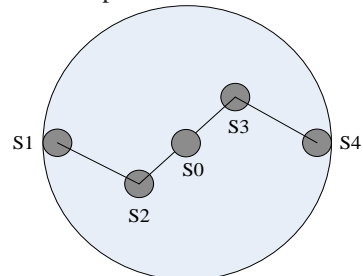


Fig.9. Five accelerometers arranged in zigzag pattern

3) Lateral movement

The lateral movement of the mass causes a lateral load on the force transducer and an axial output of the transducer due to the lateral sensitivity of the force transducer. Obviously, the effect of lateral motion can be evaluated by the ratio of the lateral acceleration to the axial acceleration of the mass. The design of the guide structure of the falling

weight and the role of ABS can greatly reduce the large mass' lateral movement. The maximum relative lateral acceleration is less than 1.0%. which is measured by a three-direction acceleration on the upper surface of the large mass in ABS. Considering that the relative lateral sensitivity of the general force transducer is less than 15%, the error introduced by the lateral motion to the force transducer sensitivity calibration in the calibration is generally less than 0.15%.

4) Measurement of the transducer's efficient mass

It is necessary to know the force transducer's efficient mass  $m_0$  in the small-amplitude impulse force calibration using the equation (3), especially in the case where  $m$  is much small.

The  $m_0$  can be measured by the sinusoidal force calibration device with laser interferometry force calibration device using the weight elimination method before the formal calibration [12]. The method can obtain the efficient mass accurately with the cooperation of different masses, and it is less affected by the transducer itself.

4. PIEZOELECTRIC TRANSDUCER CALIBRATION

One piezoelectric force transducer of KISTLER 9371 is dynamic calibrated to get its amplitude sensitivity with the high amplitude impulse force generator. The transducer and calibration ground are showed in figure 10. Experiment waveforms of 100kN are showed in figure 11, and the waveforms of force measured by laser and calibrated transducer are similar.

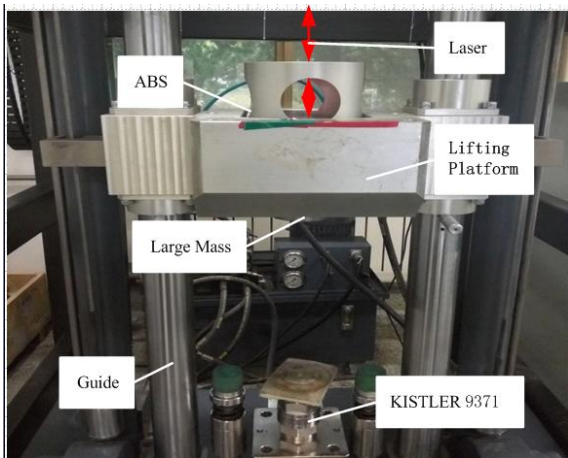


Fig.10. Calibration ground of KISTLER 9371

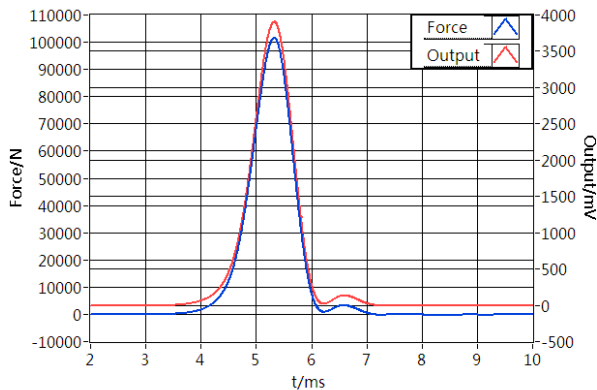


Fig.11. Experiment waveforms of KISTLER 9371 at 100kN

The calibrated results are shown in figure 12. The sensitivities' max standard deviation is 0.32%.

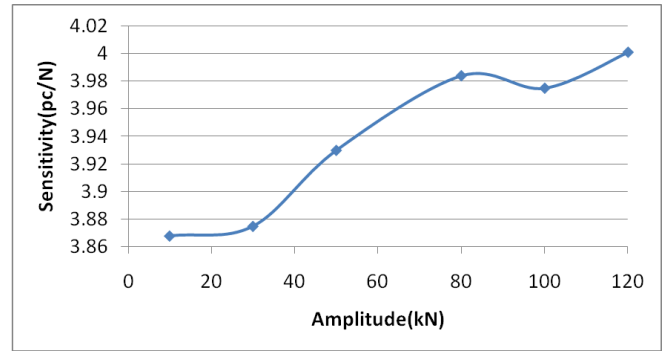


Fig.12. Calibrated sensitivities of KISTLER 9371

One ICP force transducer of PCB 208C03 is dynamic calibrated to get its amplitude sensitivity with the low amplitude impulse force generator. The effective mass of the force transducer is measured by the method mentioned above at 80Hz and is about 11.35g. Experiment waveforms of 100N are showed in figure 13. The calibrated results are shown in figure 14. The sensitivities' max standard deviation is 0.30%.

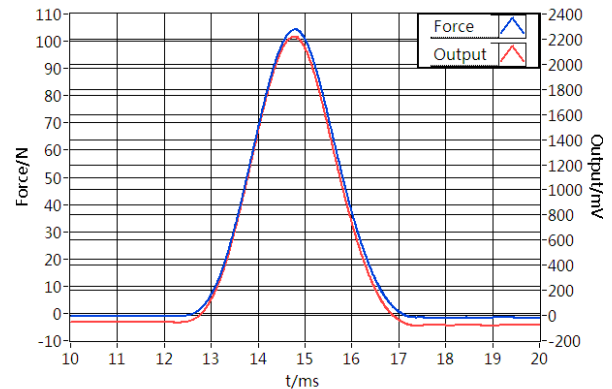


Fig.13. Experiment waveforms of PCB 208C03 at 100N

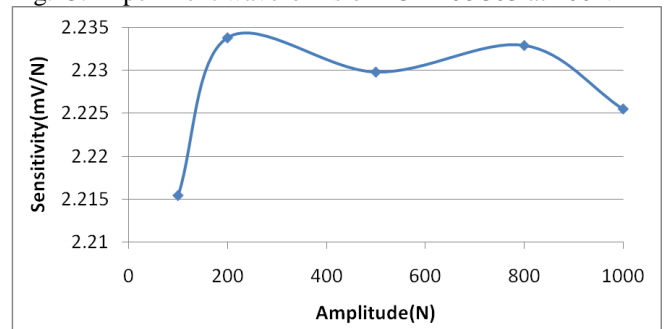


Fig.14. Calibrated sensitivities of PCB 208C03

The calibrated sensitivity's repeatability is very good for two range impulse force calibrations. Based on primary analysis the sensitivity's measurement uncertainty is less than 2% ( $k=2$ ), which is synthesized by the inertial mass measurement, the acceleration measurement by the laser vibrometer, the acceleration distribution, the lateral movement, the electric signal acquisition and the calibrated sensitivity's repeatability.

Another piezoelectric force transducer from KISTLER (9081B, 200kN) is also calibrated. The output of the transducer is significantly oscillating after the pulse, which is as the blue curve in figure 15. The smaller the pulse width



is, the greater the amplitude of the oscillation is, and the force measured by laser vibrometer does not have a similar oscillation. By monitoring the acceleration of the anvil installed by the force transducer, it is found that the anvil's acceleration has a significant oscillation starting from the impulse force. The acceleration oscillation is very similar to the oscillation of the force transducer's output after the impulse. It is presumed that this oscillation is due to the inertial force of the transducer's equivalent inertia mass under acceleration. This problem requires further analysis and study of the corresponding elimination or compensation method.

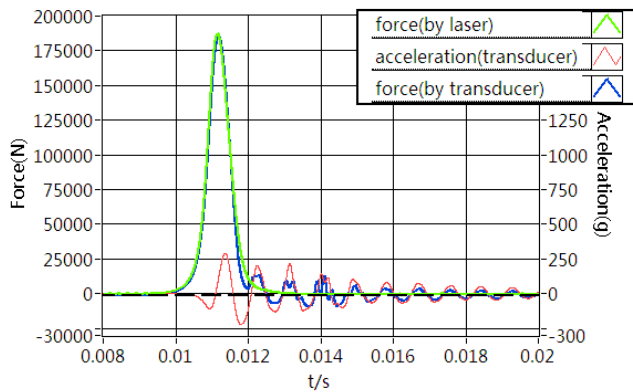


Fig.15. 9081B output's oscillation and anvil's acceleration

## 5. SUMMARY AND OUTLOOK

The good large-amplitude impulse force is realized by the mature dropped weight impact test technology and the air bearing system. The lower limit of impulse force is further extended by the double mass design. The inertial force measured by laser interferometry traces the impulse force to the basic quantity such as mass, length and time, and improves the accuracy of amplitude measurement. More researches will be done such as improvement of pulse width control capabilities, elimination or compensation of anvil's oscillation, comparison of the calibrations at different pulse widths, comparison the impulse force calibration with the sinusoidal force calibration.

## 6. REFERENCES

- [1] Jan Hjelmgren. Dynamic Measurement of Force --A Literature Survey, SP Swedish National Testing and Research Institute, SP Rapport 2002:27, (Borås 2002). ISBN 91-7848-918-0.
- [2] M. Kobusch and T. Bruns, "the New Impact Force Machine At Ptb," XVII IMEKO World Congress, June 22 – 27, 2003, Dubrovnik, Croatia, pp263-267.
- [3] M. Kobusch, T. Bruns, L. Klaus, and M. Müller, "The 250 kN primary shock force calibration device at PTB," Meas. J. Int. Meas. Confed., vol. 46, no. 5, pp. 1757–1761, 2013.
- [4] Y. Fujii, "Dynamic force calibration methods for force transducers," Conf. Rec. - IEEE Instrum. Meas. Technol. Conf., vol. 1, no. May, pp. 352–357, 2004.
- [5] Y. Iga, Y. Fujii, T. Fujyu, H. Okano, and J. D. R. Valera, "Impact Response Measurements of Force Transducers," SICE-ICASE International Joint Conference 2006 Oct. 18-21, 2006 in Bexco, Busan, Korea, pp. 1647–1651.
- [6] T. Bruns, R. Kumme, M. Kobusch, and M. Peters, "From oscillation to impact: The design of a new force calibration device at PTB," Meas. J. Int. Meas. Confed., vol. 32, no. 1, pp. 85–92, 2002.
- [7] M. Kobusch, A. Link, A. Buss, and T. Bruns, "Comparison of Shock and Sine Force Calibration Methods," IMEKO 20th TC3, 3rd TC16 and 1st TC22 International Conference Cultivating metrological knowledge 27th to 30th November, 2007. Merida, Mexico.
- [8] C. Bartoli et al., "Traceable dynamic measurement of mechanical quantities: objectives and first results of this european project," Int. J. Metrol. Qual. Eng., vol. 3, no. 3, pp. 127–135, 2013.
- [9] A. Chijioko and N. Vljajic, "Primary Sinusoidal Calibration of Force Transducers Up To 2 Kilohertz," XXI IMEKO World Congress, August 30 – September 4, 2015, Prague, Czech Republic.
- [10] N. Medina and J. de Vicente, "Force sensor characterization under sinusoidal excitations," Sensors (Switzerland), vol. 14, no. 10, pp. 18454–18473, 2014.
- [11] N. Medina, J. Robles, J. de Vicente, "Realization of sinusoidal forces at CEM". IMEKO 22nd TC3, 15th TC5 and 3rd TC22 International Conferences, Cape Town, South Africa, February 2014.
- [12] L.Zhang, Y.Wang, L.Z.Zhang, "Investigation of calibration force transducer using sinusoidal force". 9th international conference of vibration measurement by laser noncontact techniques .pp395-404, June, 2010.